RSC Advances

Volume 1 | Number 1 | Jan 2013 | Pages 1–100

RSC Advances

www.rsc.org/advances

ROYAL SOCIETY OF CHEMISTRY

www.rsc.org/advances

Cite this: DOI: 10.1039/c0xx00000x

www.rsc.org/xxxxxx

ARTICLE TYPE

Composite cathode material β-$LiVOPO_4$/$LaPO_4$ with enhanced electrochemical properties for lithium ion batteries

Chao Shen, Jun-chao Zheng*, Bao Zhang*, Ya-dong Han, Jia-feng Zhang, Lei Ming, Hui Li, Xin-bo Yuan

Received (in XXX, XXX) Xth XXXXXXXXX 20XX, Accepted Xth XXXXXXXXX 20XX

DOI: 10.1039/b000000x

---

* Corresponding author: Jun-chao Zheng, Ph.D; Tel:+86-731-88836357
E-mail address: jczheng@csu.edu.cn
* Corresponding author: Bao Zhang, Ph.D; Tel:+86-731-88836357
E-mail address: csuzjc@gmail.com

Cite this: DOI: 10.1039/c0xx00000x

www.rsc.org/xxxxxx

ARTICLE TYPE

A composite cathode material, β-$LiVOPO_4$/$LaPO_4$, is synthesized by a sol–gel method. The synthesized samples are characterized by XRD, SEM, TEM, EDS, XPS, and electrochemical tests. Results indicate that $LiVOPO_4$ has an orthorhombic structure with a Pnma space group and that $LaPO_4$ has a monazite structure with a P21/n space group. EDS and TEM results illustrate that $LaPO_4$ with typical sizes of 10–40 nm is homogeneously distributed on the surface of primary $LiVOPO_4$ particles. The synthesized β-$LiVOPO_4$/$LaPO_4$ exhibits much better electrochemical performance than bare β-$LiVOPO_4$. The β-$LiVOPO_4$/$LaPO_4$ samples delivered an initial discharge capacity of about 127.0 mAh g^{-1} at 0.1 C and possessed favorable capacities at rates of 0.5 and 1 C. Therefore, surface modification of crystalline $LaPO_4$ is an effective way to improve the electrochemical performance of β-$LiVOPO_4$.

Introduction

Lithium-ion batteries are rechargeable batteries that can be used in portable electronic devices, electric vehicles, and hybrid electric vehicles, among others, because of their high specific capacity, long cycle life, and high operating voltage.[1–2] A significant amount of research has focused on new cathode materials for lithium-ion batteries. After Goodenough's laboratory [3–5] published their research results, interest in polyanionic compounds as lithium storage electrodes for rechargeable batteries grew. Specifically, lithium transition metal phosphates, such as $LiMPO_4$ (M = Fe, Mn, or Co),[6–8] $Li_3V_2(PO_4)_3$ (M = V, Fe, or Ti),[9–11] $LiVPO_4F$,[12–13] and $LiVOPO_4$,[14] have gained extensive attention as cathode materials because of their high energy density, low cost, and excellent thermal stability.

$LiFePO_4$ is the simplest, most widely studied, and potentially most useful of these cathode materials because of its high lithium intercalation voltage (3.5 V vs. Li), high theoretical capacity of 170 mAh g^{-1}, and low cost.[15] Compared with $LiFePO_4$, lithium vanadyl phosphate ($LiVOPO_4$) exhibits higher energy density at nearly the same theoretical capacity of 166 mAh g^{-1} and a higher lithium intercalation potential of about 4 V.[14] $LiVOPO_4$ exists as α-$LiVOPO_4$ (triclinic, space group *P*-1) or β-$LiVOPO_4$ (orthorhombic, space group Pnma), which exhibit electronic conductivities of about 10^{-11} and 10^{-10} S cm^{-1}, respectively.[16–17] The orthorhombic phase has been extensively investigated because of its excellent ion-intercalation properties. However, the poor electronic and ionic conductivity has been an obstacle to the development of $LiVOPO_4$.[18–19]

Carbon coating, nano-sizing, porous structures, and morphology tailoring have been investigated to improve the performance of $LiVOPO_4$ cathode materials; however, these techniques present certain disadvantages.[20–22] Pure-phase $LiVOPO_4$, for example, is synthesized mainly through sintering in air, which results in negative effects on carbon coating and metal doping and leads to poor electrochemical performance. Hence, exploring other novel ideas to realize improved Li battery performance is necessary.

Introducing electrical additives to the surface of cathode materials is an effective way to improve the electrochemical performances of phosphate-based cathode materials.[23–25] M. M. Ren synthesized β-$LiVOPO_4$/RuO_2 composites presenting good electrochemical Li ion intercalation performance because of enhanced electrical conductivity and Li ion diffusion.[20] However, the electrical additives were only coated at a micro-scale level onto the pristine β-$LiVOPO_4$ particles so that improvements in the electrochemical performance of the lithium batteries were not very obvious. According to the reference, [26] introducing $LaPO_4$ (with good ionic conductivity) to the surface of a cathode material ($Li[Ni_{0.5}Co_{0.2}Mn_{0.3}]O_2$) is an effective way to improve the electrochemical performance of $Li[Ni_{0.5}Co_{0.2}Mn_{0.3}]O_2$.

In the present study, β-$LiVOPO_4$/$LaPO_4$ composite was synthesized and characterized, and the effects of $LaPO_4$ surface modification on the structural and electrochemical properties of the composite were investigated.

Experimental

The β-$LiVOPO_4$/$LaPO_4$ composite was synthesized via a sol–gel method. First, a stoichiometric amount of NH_4VO_3 (AR, ≥ 99.0%), $LiNO_3$ (AR, ≥ 99.0%), $(NH_4)_2HPO_4$ (AR, ≥ 99.0%), and $La(NO_3)_3$(AR, ≥ 99.0%) at 1:1.05:1.03:0.03 molar ratio were dissolved in water with magnetic stirring at 85 °C for 2 h. When the raw materials were completely dissolved, $C_2H_2O_4{\cdot}2H_2O$ (AR, ≥ 99.0%) was dissolved as both the chelating agent and reducer. Next, the mixture was continuously stirred at 85 °C until a dark blue gel formed. This gel was then dried and sintered at 450 °C for 8 h in air atmosphere to form β-$LiVOPO_4$/$LaPO_4$ composite powder. The product was spontaneously cooled to room temperature, and the β-$LiVOPO_4$/$LaPO_4$ composite was obtained. Bare β-$LiVOPO_4$ was synthesized via the same method but without $La(NO_3)_3$. The molar ratio of NH_4VO_3, $LiNO_3$, and $(NH_4)_2HPO_4$ used was 1:1.05:1.

The elemental composition of the powders was determined by XPS on an instrument (Kratos Model XSAM800) equipped with a Mg Kα achromatic X-ray source (1235.6 eV) and a JEOL-energy dispersive spectroscopy (EDS) detector. Structural and crystalline phase analyses of the products were conducted by XRD (Rint-2000, Rigaku) using Cu Kα radiation. The samples were observed by SEM, JEOL JSM-5600LV) and TEM (Tecnai G12). Elemental carbon analysis was performed using C–S analysis equipment (Eltar, Germany).

Electrochemical characterizations were performed using CR2025 coin-type cells. The composite electrodes were prepared by mixing the as-synthesized composite with carbon black and polyvinylidene difluoride at a weight ratio of 80:10:10 using NMP as the solvent. The cathode was prepared by spreading the mixture on an aluminum foil. Charge–discharge tests of the samples were performed in coin cells with cathodes and lithium anodes. After solvent evaporation, the electrodes were punched to form disks with 14 mm diameter and then dried at 120 °C for 4 h. The test cell consisted of the positive electrode and lithium foil negative electrode separated by a porous polypropylene film, and 1 mol L^{-1} $LiPF_6$ in EC: EMC: DMC (1: 1:1 v/v) as the electrolyte. The coin cells were assembled in a dry Ar-filled glove box. The cells were charged and discharged over a voltage range of 3.0–4.5 V versus a Li/Li^+ electrode at 25 °C. The cycling and charge–discharge performance of the cells was tested using an automatic galvanostatic charge–discharge unit (LAND battery cycle). Cyclic voltammograms were recorded with a scan rate of 0.1 mV s^{-1} between 3.0 and 4.5 V.

Results and discussion

The XRD patterns of the synthesized powders are shown in Fig. 1. The sharp peaks in the patterns indicate that the powders are well crystallized. The pattern of the β-$LiVOPO_4$ powders is consistent with the JCPDS data (PDF#85-2438) and literature reports.[5, 25] The main crystalline phase in both samples represents an orthorhombic structure with a Pnma space group. A subtle difference may be observed between bare β-$LiVOPO_4$ and β-$LiVOPO_4$/$LaPO_4$ from 28° to 31° (marked with an oval). The main planes of (1 2 0), (2 1 0), (0 1 2), and (-1 1 2) indicate the diffraction peaks of impurities corresponding to the peaks for $LaPO_4$, which is consistent with the JCPDS data (PDF#83-0651). These results that $LaPO_4$ has a crystalline phase and a monazite structure with a P21/n space group. The weight percentage of $LaPO_4$ in the β-$LiVOPO_4$/$LaPO_4$ composite is 4%. No other diffraction peak is found in the XRD patterns. The amount of carbon in the composites is about 1.2 wt.%, as determined by the C–S analysis method. Carbon remaining in the composite could not be detected by XRD, which indicates that the residual carbon is amorphous.

SEM images of bare β-$LiVOPO_4$ and β-$LiVOPO_4$/$LaPO_4$ are shown in Fig. 2. The surfaces of bare β-$LiVOPO_4$ particles [Figs. 2(a) and 2(b)] are slightly smoother than those of β-$LiVOPO_4$/$LaPO_4$ [Figs. 2(c) and 2(d]. In addition, the particle sizes of β-$LiVOPO_4$/$LaPO_4$ sample are much smaller than those of bare β-$LiVOPO_4$, which is beneficial to intercalation and de-intercalation of Li ions over short paths. Moreover, β-$LiVOPO_4$/$LaPO_4$ has more pores than β-$LiVOPO_4$; these pores cause an increase in the specific area of the former. The surface areas of β-$LiVOPO_4$ and β-$LiVOPO_4$/$LaPO_4$ are 3.012 and 3.898 m^2 g^{-1}, respectively.

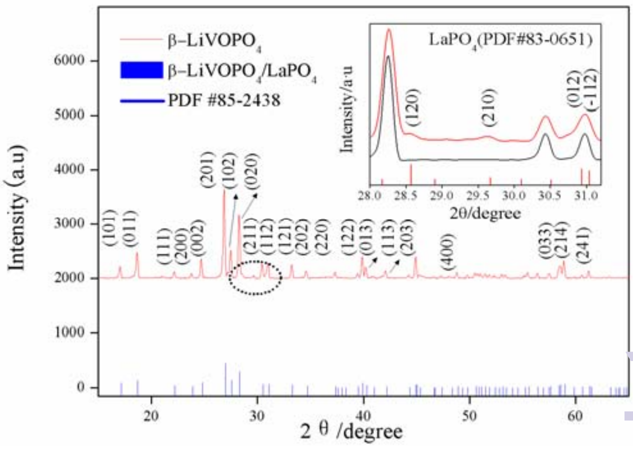

Fig.1 XRD patterns of the synthesized samples

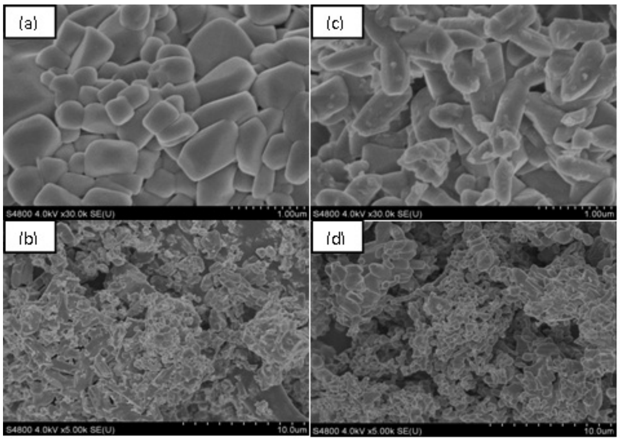

Fig.2 (a, b) SEM images of β-$LiVOPO_4$;

(c, d) SEM images of β-$LiVOPO_4$/$LaPO_4$

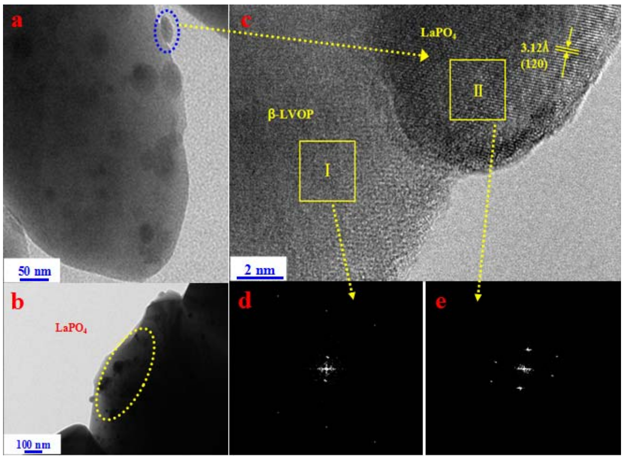

Fig.3 (a, b) TEM image of β-$LiVOPO_4$/$LaPO_4$ composite material (c) The local amplification of one of selected $LaPO_4$ site (d, e) Fourier transform (FFT) of the selected areas

HRTEM images of β-$LiVOPO_4$/$LaPO_4$ are shown in Fig. 3. As seen in Figs. 3(a) and 3(b), the β-$LiVOPO_4$ particle is surrounded by $LaPO_4$ nanoparticles, and the particle size of

$LaPO_4$ is within 10–40 nm. The presence of $LaPO_4$ as observed in the present study is different from that described in previous literature reports, in which $LaPO_4$ may be observed as a thin amorphous layer on the surface of the particles.[25] To verify the characteristics of $LaPO_4$ modification, local amplification of one of the modification sites (marked with a blue circle) was performed, as shown in Fig. 3(c). One type of lattice fringe was found in the $LaPO_4$ modification site [right section in Fig. 3(c)]. The lattice fringe is attributed to $LaPO_4$ with an inter-planar spacing of 3.12 Å, which corresponds to the (1 2 0) lattice plane. These results indicate that crystalline-phase$LaPO_4$ particles are distributed on the surface of β-$LiVOPO_4$ particles, which is consistent with the XRD results. Figs. 3(d) and 3(e) reveal the Fourier transform (FFT) of the selected areas. The FFT image in Fig. 3(d) shows the diffraction spots of β-$LiVOPO_4$, while the FFT image in Fig. 3(e) corresponds to the diffraction spots of $LaPO_4$.

To analyze the uniformity of element distribution in $LaPO_4$, EDS analysis was carried out. Fig. 4 shows the EDS patterns of vanadium, phosphorus, and lanthanum in the β-$LiVOPO_4$/$LaPO_4$ sample. Vanadium and phosphorus are uniformly distributed in the sample, and lanthanum is homogeneously dispersed on the surface of primary particles. These results clearly illustrate that crystalline $LaPO_4$ is homogeneously distributed on the surface of β-$LiVOPO_4$ primary particles.

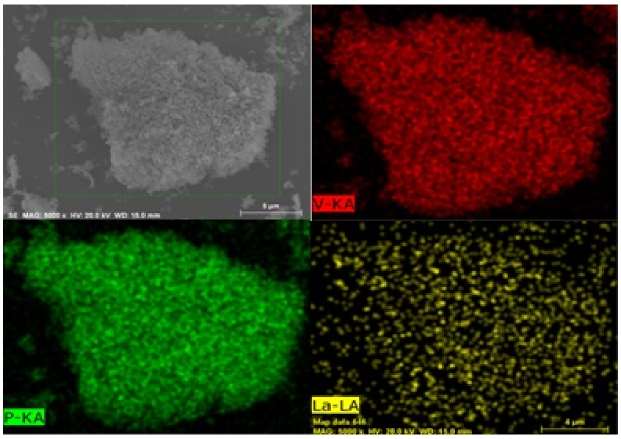

Fig.4 X-ray spectroscopy (EDS) analysis of vanadium, phosphorus and lanthanum for β-$LiVOPO_4$/$LaPO_4$ composite material

The XPS spectra of β-$LiVOPO_4$/$LaPO_4$ sample are shown in Fig. 5. Peaks appearing at 54.96, 130.70, 531.80, 517.28, and 853.08 eV can be assigned to Li1s, P2p, O1s, V2p, and La3d3, respectively. The test values are fairly consistent with the reference,[27] which reports that Li^+, P^{5+}, O^{2-}, and La^{3+} cations exhibit characteristic peaks of Li1s, P2p, O1s, and La3d3 at 54.9, 130.6, 531.8, and 853.0 eV, respectively. In addition, according to another reference,[28] V^{4+} (VO_2) cations exhibit a peak of V2p at 517.3 eV. These results reveal that the valence state of vanadium in the external surface area of the sample is +4 and that of lanthanum is +3. The results are consistent with the discussion above.

The charge/discharge curves of Li/β-$LiVOPO_4$ and Li/β-$LiVOPO_4$/$LaPO_4$ cells at different rates of 0.1, 0.25, 0.5, and 1 C (160 mA g^{-1}) in the voltage range of 3.0–4.5 V at 25 °C are illustrated in Fig. 6(a). The Δ*V* of charge/discharge plateaus in the curves of the β-$LiVOPO_4$/$LaPO_4$ cell is much smaller than that of bare β-$LiVOPO_4$. In addition, the initial discharge capacities of β-$LiVOPO_4$ at rates of 0.1, 0.25, 0.5, and 1 C are about 109.1, 94.3, 76.7, and 54.6 mAh g^{-1}, respectively, whereas those of β-$LiVOPO_4$/$LaPO_4$ are about 127.0, 120.0, 103.6, and 83.0 mAh g^{-1}, respectively. Apparently, the rate capacity of β-$LiVOPO_4$/$LaPO_4$ is much better than that of β-$LiVOPO_4$.

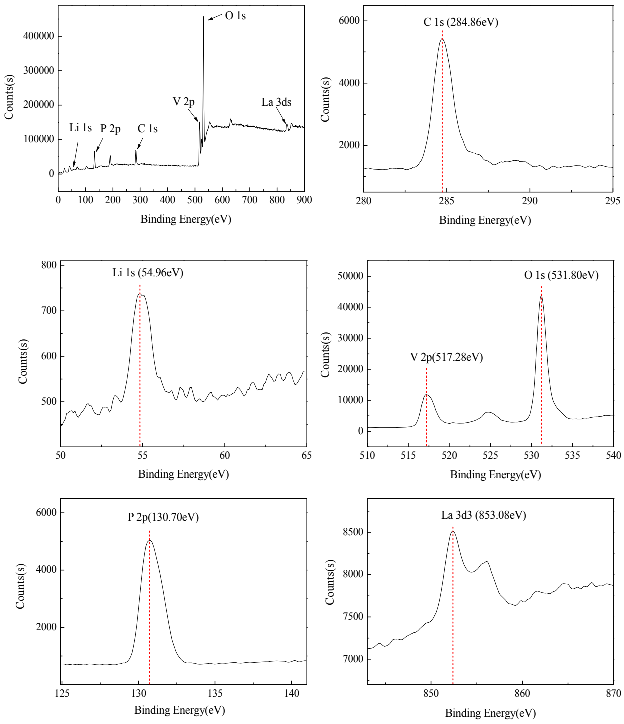

Fig.5 X-ray photoelectron(XPS) spectra of β-$LiVOPO_4$/$LaPO_4$ composite material

Based on Fig. 6(b), the discharge capacities of β-$LiVOPO_4$ at rates of 0.1, 0.25, 0.5, and 1 C are about 99.2, 84.5, 63.3, and 36.0 mAh g^{-1} after 30 cycles, which indicates that the cell respectively retains 90.9%, 89.6%, 82.5%, and 65.9% of its initial discharge capacity,. Compared with β-$LiVOPO_4$, the discharge capacities of β-$LiVOPO_4$/$LaPO_4$ at rates of 0.1, 0.25, 0.5, and 1 C are about 125.0, 116.0, 97.0, and 73.6 mAh g^{-1} after 30 cycles, and the cell respectively retains 98.4%, 96.7%, 93.6%, and 73.6% of its initial discharge capacity. Thus, the capacity retention of β-$LiVOPO_4$/$LaPO_4$ displays greater advantages compared with that of bare β-$LiVOPO_4$ even at higher rates.

From the discussion above, we can draw the conclusion that the composite cathode material β-$LiVOPO_4$/$LaPO_4$ shows better electrochemical performance than β-$LiVOPO_4$ because of introduction of the ionic conductor $LaPO_4$ to the 3D network between β-$LiVOPO_4$ primary particles.

Fig. 6(c) shows the cyclic voltammetry curves of β-$LiVOPO_4$ and β-$LiVOPO_4$/$LaPO_4$ at a scan rate of 0.1 mV s^{-1} between 3.0 and 4.5 V. The redox processes of β-$LiVOPO_4$ and β-$LiVOPO_4$/$LaPO_4$ occur at 3.822/4.160 V and 3.839/4.066 V, respectively, which may be assigned to the $V^{4+/5+}$ couples and attributed to $LiVOPO_4$.The voltage gap between the redox peaks of β-$LiVOPO_4$/$LaPO_4$ is obviously much smaller than that of bare β-$LiVOPO_4$, which indicates that β-$LiVOPO_4$/$LaPO_4$ presents much better reversibility for Li^+ extraction/insertion. These results are in accordance with the charge and discharge curves obtained previously.

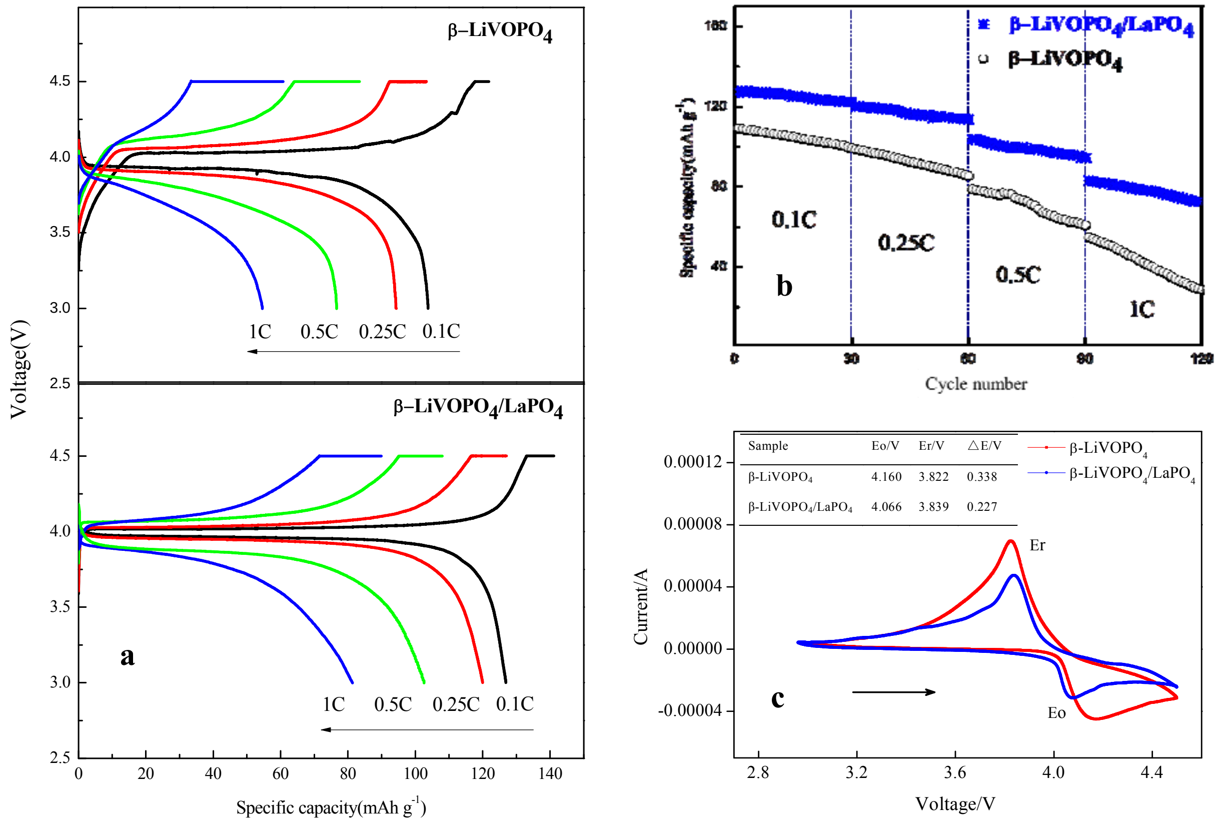

Fig.6 (a, b) Charge/discharge profiles and cycling performance of β-$LiVOPO_4$ and β-$LiVOPO_4$/$LaPO_4$ cathode; (c) Cyclic voltammetry curves for β-$LiVOPO_4$ and β-$LiVOPO_4$/$LaPO_4$ cathode at a scan rate of 0.1 mV s^{-1}

Conclusions

β-$LiVOPO_4$/$LaPO_4$ was synthesized via the sol–gel method, and crystalline $LaPO_4$ was successfully distributed on the surface of β-$LiVOPO_4$ primary particles. Introduction of the ionic conductor $LaPO_4$ to the 3D network between β-$LiVOPO_4$ primary particles and the small particle and pore structure of the matrix enhanced the discharge capacity, cyclic stability, and capacity retention of the resultant composite compared with those of bare β-$LiVOPO_4$. Hence, introduction of $LaPO_4$ to β-$LiVOPO_4$ is an effective way to enhance the electrochemical performance of $LiVOPO_4$.

Acknowledgements

This study was supported by National Natural Science Foundation of China (Grant No. 51302324 and 51272290) and the Fundamental Research Funds for the Central Universities of Central South University (2013zzts028).

Notes and references

School of Metallurgy and Environment, Central South University, Changsha 410083, P.R. China
[*] Corresponding author: Jun-chao Zheng, Ph.D; Tel:+86-731-88836357
E-mail address: jczheng@csu.edu.cn
[*] Corresponding author: Bao Zhang, Ph.D; Tel:+86-731-88836357
E-mail address: csuzjc@gmail.com

1 P. G. Bruce, B. Scrosati and J. M. Tarascon, *Angew. Chem. Int. Ed.*, 2008, **47,** 2930.
2 H. Li, Z. X. Wang, L. Q. Chen and X. J. Huang, *Adv. Mater.*, 2009, **21**, 4953.
3 A. K. Padhi, K. S. Najundaswamy and J. B. Goodenough, *J. Electrochem. Soc.*, 1997, **144**, 1188.
4 A. K. Padhi, K. S. Najundaswamy, C. Masquelier, S. Okada and J. B. Goodenough, *J. Electrochem. Soc.*, 1997, **144**, 1609.
5 K. S. Nanjundaswamy, A. K. Padhi, J. B. Goodenough, S. Okada, H. Ohtsuka, H. Arai and J. Yamaki, *Solid State Ionics*, 1996, **92**, 1.
6 M. Konarova and I. Taniguchi, *J. Power Sources*, 2010, **195**, 3661.
7 D. W. Han, Y. M. Kang, R. Z. Yin, M. S. Song and H. Kwon, *Commun.* 2009, **11**, 137.

8 D. Wang, H. Buqa, M. Crouze, G. Deghenghi, T. Drezenb, I. Exnar, N. Kwon, J.H. Miners, L. Poletto and M. Gratzel. *J. Power Sources*, 2009, **189**, 624.

9 J. C. Zheng, X. H. Li and Z. X. Wang, *J. Power Sources*, 2010, **195**, 2935.

10 A. S. Andersson, B. Kalska, P. Jonsson, L. Haggstrom, P. Nordblad, R. Tellgren and J. O. Thomas, *J. Mater. Chem.,* 2000, **10**, 2542.

11 C. M.Burba and R. Frech, *Solid State Ionics*, 2006, **177**, 1489.

12 S. K. Zhong, Z. L. Yin, Z. X. Wang and Q. Y. Chen, *Journal of Central South University of Technology*,2007, **14**, 340.

13 B. Zhang, Y. D. Han, J. C. Zheng, C. Shen, L. Ming and J. F. Zhang, *Journal of Power Sources*, 2004, **264**, 123.

14 K. L. Harrison, A. Manthiram*, Chem. Mater.* 2013, **25**, 1751.

15 J. C. Zheng, X. H. Li, Z. X. Wang, H. J. Guo and S. Y. Zhou. *J. Power Sources*, 2008, **184**, 574.

16 J. Barker, M. Y. Saidi and J. L. Swoyer, *J. Electrochem. Soc.,* 2004, **151**, A796.

17 T. A. Kerr, J. Gaubicher and L. F. Nazar, *Electrochem. Solid-State Lett.,* 2000, **3**, 460.

18 K. Saravanan, H. S. Lee, M. Kuezma, J. J. Vittal and P. Balaya, *J. Mater. Chem.,* 2011, **21**, 10042.

19 D. Morgan, G. Ceder, M. Y. Saidi, J. Swoyer, H. Huang and G. Adamson, *Chem. Mate.,* 2002, **14**, 4684.

20 M. M. Ren, Z. Zhou, L. W. Su and X. P. Gao, *J. Power Sources*, 2009, **189**, 786.

21 B. M. Azmi, T. Ishihara, H. Nishiguchi and Y. Takita, *J. Power Sources*, 2005, **146**, 525.

22 B. M. Azmi, H. S. Munirah, T. Ishihara and Y. Takita, *Ionics*, 2005, **11**, 402.

23 S. H. Lim and J. Cho, *Electrochemistry Communications,* 2008, **10,** 1478.

24 P. Mohan and G. P. Kalaignann, *Ceramics International, 2014,* **40**, 1415.

25 B. Zhang, C. Shen, J. C. Zheng, Y. D. Han, J. F. Zhang, L. Ming, J. L. Wang and S. E. Qin, H. Li, *Journal of The Electrochemical Society*, 2014, **161**, A748.

26 H. G. Song, K-S Park and Y. J. Park, *Solid State Ionics,* 2012, **225**, 532.

27 Handbook of Monochromatic XPS Spectra - Vol. 1 - The Elements and Native Oxides B. V. Crist, XPS International, Inc., 1999.

28 J. C. Zheng, X. H. Li, Z. X. Wang, H. J. Guo, Q. Y. Hu and W. J. Peng, *J. Power Sources*, 2009, **189**, 476.